Detection of subcellular nitric oxide in the mitochondria by a pyrylium probe: assays in cell cultures and peripheral blood

Ignacio Muñoz Resta,[a] Begoña Bedrina,[a] Elena Martínez-Planes,[b] Alfredo Minguela[b] and Francisco Galindo*[a]

a. Departamento de Química Inorgánica y Orgánica, Universitat Jaume I, Av. V. Sos Baynat s/n, 12071, Castellón, Spain. E-mail: francisco.galindo@uji.es

b. Servicio de Inmunología, Hospital Universitario Virgen de la Arrixaca, El Palmar, 30120, Murcia, Spain.

Abstract. Fluorescent probes for the detection of intracellular nitric oxide (NO) are abundant, but those targeted to the mitochondria are scarce. Among those molecules measuring mitochondrial NO (mNO), the majority use the triphenylphosphonium (TPP) cation as a vector to reach such organelle. Here we describe a simple molecule (mtNOpy) based on the pyrylium structure, made in few synthetic steps, capable to detect selectively NO (aerated medium) over other reactive species. The calculated detection limit for mtNOpy is 88 nM. The main novelty of this probe is that its simple molecular architecture can act both as fluorogenic and as mitochondriotropic, without using TPP. mtNOpy has been tested in two different scenarios: (a) on a controlled environment of cell line cultures (human colon carcinoma HT-29 cells and mouse macrophage RAW 264.7 cells), using confocal laser scanning microscopy, and (b) on a much more complex sample of peripheral blood, using flow cytometry. In the first context, mtNOpy has been found to be responsive (turn-on fluorescence) to exogenous and endogenous NO stimulus (via SNAP donor and LPS stimulation, respectively). In the second area, mtNOpy has been able to discriminate between NO-generating phagocytes (neutrophils and monocytes) from other leukocytes (NK, B and T cells).

Keywords: nitric oxide; mitochondria; pyrylium; fluorescence; probes; microscopy; cytometry

Introduction

Mitochondria are involved in the production of energy via the oxidative phosphorylation process and recently have been recognized as key elements in the immune response to pathogens and cancer.[1–5]. The details of some pathological processes linked to mitochondrial function are still elusive. The knowledge about mitochondrial machinery has been gained through decades thanks to the use of several approaches. Fluorescence-based strategies have been especially important due to the high spatiotemporal resolution of confocal microscopy or to the high throughput screening capacity of flow cytometry, for instance.[6,7]. Thus, the development of molecular dyes or nanomaterials to interrogate the mitochondria has grown enormously in recent years.[8–10] However, reaching a specific organelle inside the cell requires a proper design of the molecule or material. One method to direct a sensory system to the mitochondria is the use of the triphenylphosphonium (TPP) cation due to the high affinity of this moiety to the aforementioned organelle.[11–18] The introduction of this group in the architecture of the probe often requires synthetic detours that compromise the success of the preparation process or the final amount of available probe.

We have recently shown that minimalistic styrylpyrylium dyes, delocalized lipophilic compounds (DLC) obtained in three synthetic steps, can reach the mitochondria of Hep3B hepatocarcinoma cells very efficiently.[19] A paradigmatic example of them is compound **1** depicted in **Chart 1**, which, on the contrary to TPP, is intrinsically fluorescent. We reasoned that simple modification of **1** with appropriate reactive groups would lead to molecules with the potential to generate fluorescence inside mitochondria of live cells upon the correct stimulus. Following our interest in the study of nitric oxide (NO) probes,[20–22] we hypothesized that an amine group would react with NO (in aerated medium) leading to a fluorescence response. NO is one of the most

intriguing and studied species in the last decades, having roles at numerous biological levels.[23] The synthetic approaches to develop NO probes are varied.[24–38] One of them involves the use of primary amines that, upon the appropriate conditions, can suffer a deamination reaction and, concomitantly, a fluorescent turn-on response.[22,39,40] Thus, probe **2** was synthesized (**Chart 1**), differing from **1** only in the presence of an amino group. The presence of this group not only would impart the desired reactivity to the indicator but also would quench the emission of the probe. Although the number of NO probes reported so far is numerous, those specifically targeting mitochondrial NO (mNO) are scarce, and most of them use the TPP directing group.[41–45] There are few fluorescent probes for mNO not relying on this vector.[46–49] Here we would like to report the sensing ability of probe **2** to mNO, as demonstrated in cultured cells (HT-29 human colon cancer and RAW 264.7 murine macrophages). We have given a step beyond cell cultures and compound **2** has been challenged to discriminate NO-producing phagocytes (neutrophils and monocytes) from lymphocytes (NK, B and T cells) in a real sample of peripheral blood.

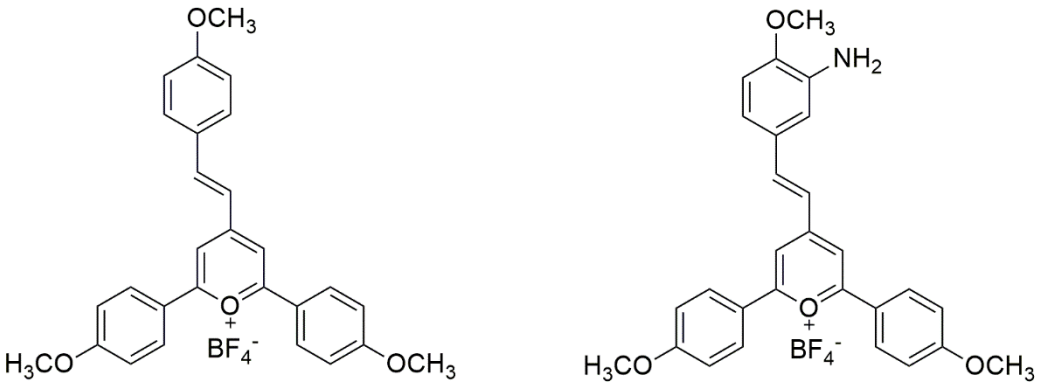

Chart 1. Mitochondrial marker **1** and its analogue **2** (mtNOpy) designed to sense nitric oxide in the mitochondria.

Experimental methods

Materials and instruments. All commercially available reagents and solvents were used as received. ^{1}H and ^{13}C NMR spectra were measured with a Bruker Advance III HD spectrometer (400 MHz for ^{1}H and 101 MHz for ^{13}C). High-resolution mass spectra were performed on a Waters Q-Tof Premier mass spectrometer with an electrospray source. UV-vis spectra were obtained with a Cary 60 UV-vis spectrophotometer, using quartz cuvettes with 1 cm path length and 3 mL volume. Steady-state emission was recorded with an Agilent Cary-Eclipse spectrofluorometer. Cellular images were obtained using a Leica TCS SP8 inverted confocal laser-scanning microscope. Images were processed with Fiji; a subtract background function was employed with a sliding paraboloid function of 50 pixels followed by a median filtering function used with a radius of 1 pixel. Flow cytometric analysis was recorded on BD Accuri™ C6 flow cytometer.

Measurements. The complete details for experimental procedures are provided in the supporting information.

Synthesis and characterization of compounds 2-4. 2,6-bis(4-methoxyphenyl)-4-methylpyrylium tetrafluoroborate was synthesized following the procedure we described previously.[19]

(E)-4-(4-methoxy-3-nitrostyryl)-2,6-bis(4-methoxyphenyl)pyrylium tetrafluoroborate. (red solid, 0.22 g, 63 % yield). A suspension of 2,6-bis(4-methoxyphenyl)-4-methylpyrylium tetrafluoroborate (0.25 g, 0.63 mmol) and 4-methoxy-3-nitrobenzaldehyde (0.17 g, 0.95 mmol) in acetic acid (10 ml) was heated to reflux (a dark solution was formed) for 24 hours. After cooling down to room temperature, the crude reaction was poured into 200 ml of diethyl ether, and the red precipitate was recovered by filtration, washed, and dried under vacuum.

^{1}H NMR (400 MHz, CD_3CN) δ 8.28 – 8.15 (m, 6 H), 8.14 (s, 2H), 8.01 (dd, J = 8.9, 2.2 Hz, 1H), 7.39 (d, J = 9.2 Hz, 1H), 7.35 (d, J = 16.7 Hz, 1H), 7.27 – 7.19 (m, 4H), 4.04 (s, 3H), 3.97 (s, 3H). ^{13}C NMR (101 MHz, CD_3CN) δ 169.84, 166.42, 156.25, 145.49, 135.84, 131.44, 131.44, 122.38, 116.63, 116.18, 113.31, 57.97, 56.90, 56.90. HRMS (ESI-TOF)$^+$ calculated for $C_{28}H_{24}NO_6^+$ (M^+) (m/z): 470.1598; experimental (M^+) (m/z): 470.1595.

Compound 2. *(E)-4-(3-amino-4-methoxystyryl)-2,6-bis(4-methoxyphenyl)pyrylium tetrafluoroborate* (dark red solid, 0.16 g, 97 % yield). In a two-neck round-bottom flask, $SnCl_2.2H_2O$ (0.43 g, 1.89 mmol) was dissolved in acetic acid (10 ml) with HCl (0.29 ml, 9.42 mmol) under continuous stirring and N_2 atmosphere. (E)-4-(4-methoxy-3-nitrostyryl)-2,6-bis(4-methoxyphenyl)pyrylium tetrafluoroborate (0. 18 g, 0.31 mmol) was then added, and the reaction was heated to reflux for 2 hours. After cooling down to room temperature, the formed precipitate was recovered by filtration, washed with acetic acid, and dried under vacuum.

^{1}H NMR (400 MHz, DMSO-d_6) δ 8.57 (s, 2H), 8.47 (d, J = 15.9 Hz, 1H), 8.34 (d, J = 8.9 Hz, 4H), 7.30 – 7.22 (m, 5H), 7.20 – 7.12 (m, 2H), 7.04 (d, J = 8.2 Hz, 1H), 3.94 (s, 6H), 3.90 (s, 3H). ^{13}C NMR (101 MHz, DMSO-d_6) δ 166.80, 164.24, 161.37, 151.30, 149.05, 130.15, 128.00, 121.62, 115.42, 111.62, 55.99, 55.82. HRMS (ESI-TOF)$^+$ calculated for $C_{28}H_{26}NO_4^+$ (M^+) (m/z): 440.1856; experimental (M^+) (m/z): 440.1858.

(E)-2,6-bis(4-methoxyphenyl)-4-(3-nitrostyryl)pyrylium tetrafluoroborate. (dark brown solid, 0.21 g, 79 % yield) A suspension of 2,6-bis(4-methoxyphenyl)-4-methylpyrylium tetrafluoroborate (0.20 g, 0.51 mmol) and 3-nitrobenzaldehyde (0.12 g, 0.76 mmol) in acetic acid (10 ml) was heated to reflux (a dark solution was formed) for 24 hours. After cooling down to room temperature, the crude reaction was poured into 200 ml of diethyl

ether, and the red precipitate was recovered by filtration, washed, and dried under vacuum.

^{1}H NMR (400 MHz, CD_3CN) δ 8.61 (t, J = 2.0 Hz, 1H), 8.35 (ddd, J = 8.2, 2.2, 0.9 Hz, 1H), 8.33 – 8.24 (m, 7H), 8.15 (d, J = 7.8 Hz, 1H), 7.78 (t, J = 8.0 Hz, 1H), 7.57 (d, J = 16.3 Hz, 1H), 7.29 – 7.23 (m, 4H), 3.98 (s, 6H). ^{13}C NMR (101 MHz, CD_3CN) δ 170.37, 166.62, 162.07, 144.71, 135.66, 131.79, 131.62, 126.76, 124.07, 122.28, 116.71, 113.87, 56.94. HRMS (ESI-TOF)$^{+}$ calculated for $C_{27}H_{22}NO_5^{+}$ (M^{+}) (m/z): 440.1492; experimental (M^{+}) (m/z): 440.1491.

C**ompound 3**. *(E)-4-(3-aminostyryl)-2,6-bis(4-methoxyphenyl)pyrylium tetrafluoroborate* (red solid, 0.09 g, 95 % yield). In a two-neck round-bottom flask, $SnCl_2.2H_2O$ (0.26 g, 1.12 mmol) was dissolved in acetic acid (10 ml) with HCl (0.18 ml, 5.87 mmol) under continuous stirring and N_2 atmosphere. (E)-2,6-bis(4-methoxyphenyl)-4-(3-nitrostyryl)pyrylium tetrafluoroborate (0.10 g, 0.19 mmol) was then added, and the reaction was heated to reflux for 2 hours. After cooling down to room temperature, the formed precipitate was recovered by filtration, washed with acetic acid, and dried under vacuum.

^{1}H NMR (400 MHz, DMSO-d_6) δ 8.69 (s, 2H), 8.47 (d, J = 16.1 Hz, 1H), 8.39 (d, J = 8.8 Hz, 4H), 7.43 (d, J = 16.1 Hz, 1H), 7.31 (d, J = 9.0 Hz, 4H), 7.26 (d, J = 7.8 Hz, 1H), 7.11 – 7.00 (m, 2H), 6.84 (d, J = 8.0 Hz, 1H), 3.96 (s, 6H). ^{13}C NMR (101 MHz, DMSO-d_6) δ 168.53, 164.86, 129.49, 120.61, 114.60, 111.39, 54.40. HRMS (ESI-TOF)$^{+}$ calculated for $C_{27}H_{24}NO_3^{+}$ (M^{+}) (m/z): 410.1751; experimental (M^{+}) (m/z): 410.1750.

(E)-4-(2-methoxy-5-nitrostyryl)-2,6-bis(4-methoxyphenyl)pyrylium tetrafluoroborate (red solid, 0.27 g, yield 76 %). A suspension of 2,6-bis(4-methoxyphenyl)-4-

methylpyrylium tetrafluoroborate (0.25 g, 0.63 mmol) and 2-methoxy-5-nitrobenzaldehyde (0.17 g, 0.95 mmol) in acetic acid (10 ml) was heated to reflux (a dark solution was formed) for 24 hours. After cooling down to room temperature, the crude reaction was poured into 200 ml of diethyl ether, and the red precipitate was recovered by filtration, washed, and dried under vacuum.

^{1}H NMR (400 MHz, CD_3CN) δ 8.63 (d, J = 2.8 Hz, 1H), 8.42 – 8.34 (m, 2H), 8.31 – 8.25 (m, 4H), 8.23 (s, 2H), 7.69 (d, J = 16.4 Hz, 1H), 7.29 (d, J = 9.3 Hz, 1H), 7.27 – 7.22 (m, 4H), 4.13 (s, 3H), 3.98 (s, 6H). ^{13}C NMR (101 MHz, CD_3CN) δ 170.05, 166.50, 164.79, 162.68, 142.67, 141.07, 131.56, 129.31, 127.43, 126.63, 124.89, 122.33, 116.64, 113.69, 113.63, 57.87, 56.92. HRMS (ESI-TOF)$^{+}$ calculated for $C_{28}H_{24}NO_6^{+}$ (M^{+}) (m/z): 470.1598; experimental (M^{+}) (m/z): 470.1615.

C**ompound 4**. *(E)-4-(5-amino-2-methoxystyryl)-2,6-bis(4-methoxyphenyl)pyrylium tetrafluoroborate* (red solid, 0.17 g, 90 % yield). In a two-neck round-bottom flask, $SnCl_2.2H_2O$ (0.49 g, 2.15 mmol) was dissolved in acetic acid (10 ml) with HCl (0.33 ml, 10.8 mmol) under continuous stirring and N_2 atmosphere. (E)-4-(2-methoxy-5-nitrostyryl)-2,6-bis(4-methoxyphenyl)pyrylium tetrafluoroborate (0.2 g, 0.36 mmol) was then added, and the reaction was heated to reflux for 2 hours. After cooling down to room temperature, the formed precipitate was recovered by filtration, washed with acetic acid, and dried under vacuum.

^{1}H NMR (400 MHz, MeOD) δ 8.57 (d, J = 16.4 Hz, 1H), 8.54 (s, 2H), 8.46 – 8.40 (m, 4H), 7.95 (d, J = 2.7 Hz, 1H), 7.79 (d, J = 16.3 Hz, 1H), 7.59 (dd, J = 8.9, 2.7 Hz, 1H), 7.38 (d, J = 9.0 Hz, 1H), 7.35 – 7.29 (m, 4H), 4.14 (s, 3H), 4.03 (s, 6H). ^{13}C NMR (101 MHz, MeOD) δ 170.47, 166.98, 163.49, 160.82, 142.00, 131.71, 128.53, 127.37, 126.33, 125.64, 125.28, 122.78, 116.80, 114.52, 113.51, 57.05, 56.60. HRMS (ESI-

TOF)$^+$ calculated for $C_{28}H_{26}NO_4^+$ (M^+) (m/z): 440.1856; experimental (M^+) (m/z): 440.1854.

Results and discussion

Probe **2** was synthesized starting from readily available commercial products (*p*-methoxyacetophenone and triethylorthoformate) as depicted in **Scheme S1** shown in the Electronic Supporting Information (ESI) file, in five synthetic steps. The probe was purified easily by precipitation in diethyl ether, thus avoiding chromatographic techniques. As expected, the unreacted probe is almost non-emissive, likely due to an intramolecular photoinduced electron transfer (PET) process occurring from the amino group to the pyrylium core. Upon exposure to excess NO (in aerated medium to generate the surrogate reactive nitrosating species N_2O_3), the fluorescence is strongly turned-on (120 times) affording an orange color emission (585 nm) (**Figure S1**). In **Table S1** the pertinent spectroscopic data of **2** and its reaction product with NO are compiled. This reaction takes place within minutes (**Figure S2**) and the corresponding calibration curve (3σ/k) affords a detection limit of 88 nM, in line with other probes for NO described so far (**Figure 1**). Moreover, the emission of both **2** and **2** + NO is not affected by pH changes in the range pH 4-8 (**Figure S3**). Regarding selectivity, when **2** is exposed to other reactive oxygen and nitrogen species (RNS and ROS, respectively) of biological relevance, the response is negative (species tested: hydrogen peroxide, nitrite, nitrate, superoxide radical anion, hydroxyl radical, singlet oxygen and hypochlorite) (**Figure 2**). Additionally, exposure to dehydroascorbic acid (DHA) also results in a negative response. This species has been included in the selectivity test since it is a well-known and sometimes overlooked interference.[50] The product of the reaction between **2** and NO (aerated medium) is **1**. This must occur *via* a deamination process, like the ones occurring for other described NO-reactive systems.[22,39,40,51] The occurrence

of this process seems to be confirmed employing HRMS (peak at m/z 425.1752) (**Figure S4**) and by the fact that emission of reacted **2** coincides with the fluorescence spectrum of **1** (585 nm) (**Figure S5**). Nevertheless, a comprehensive mechanistic study should be carried out in order to elucidate the exact details of the signaling process.

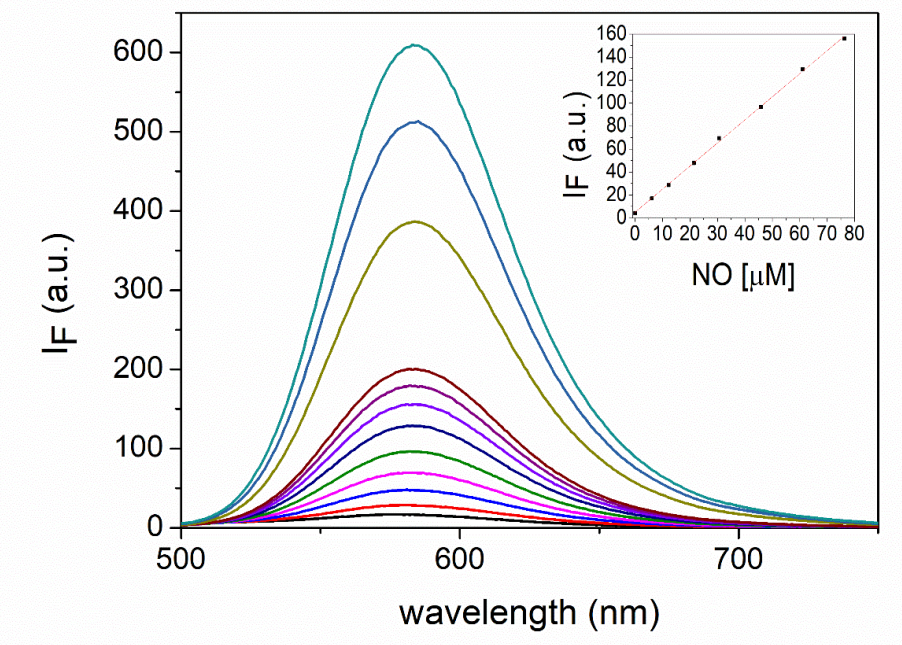

Figure 1. Changes in emission spectra of 10 μM solutions of **2** after the addition of different amounts of NO (from 0 to 1000 μM) in PBS 10 mM (pH 7.4, 20% DMF as a cosolvent). λ_{exc} was set at 480 nm. Inset: fluorescence intensity at 585 nm vs NO concentration from 0 to 80 μM. Spectra were recorded 20 minutes after the addition of NO.

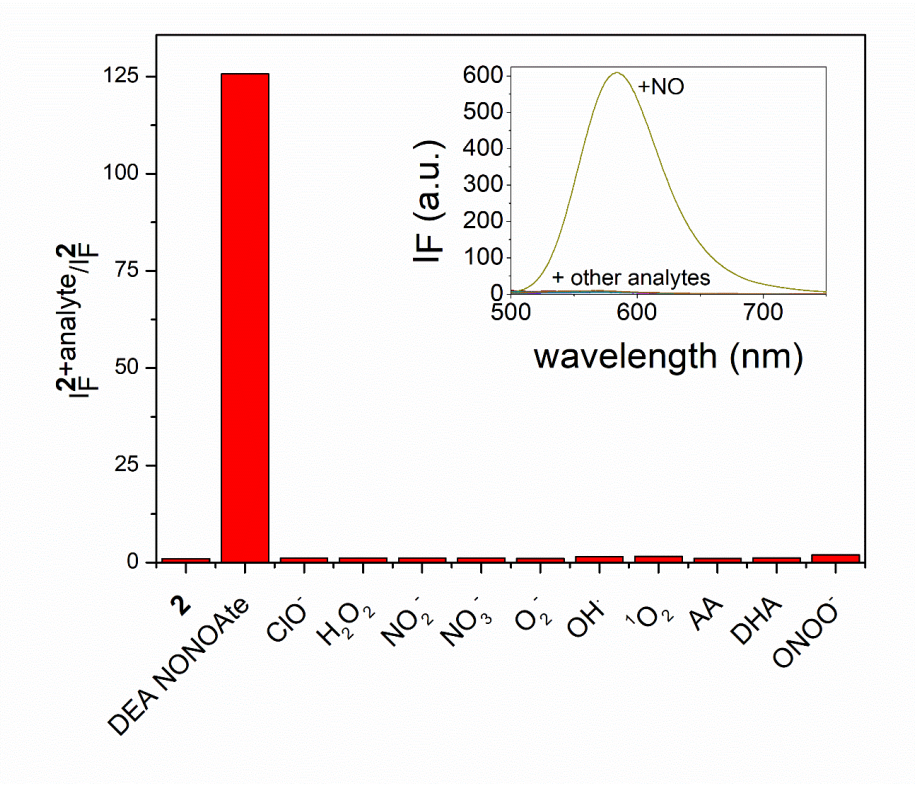

Figure 2. Changes in the fluorescence intensity at 585 nm of 10 µM solutions of **2** after the addition of 50 equivalents of different reactive nitrogen, oxygen species, ClO^-, AA and DHA in PBS 10 mM (pH 7.4, 20 % DMF as a cosolvent). λ_{exc} was set at 480 nm. Spectra were recorded 20 minutes after the addition of the analytes. Inset: emission spectra.

In order to check the need for an amino group and a methoxy group placed in *ortho* position, other molecules, with small variations in the molecular architecture, were assayed (**Chart 2**). For instance, a model dye lacking the methoxy group was synthesized (molecule **3**). As it can be seen in **Figure S6**, the response to NO (aerated medium) is very weak, which demonstrates that the aryl ring must be activated with an electron-donating group. Also, molecule **4** was made, having the MeO- group in *para* position relative to the $-NH_2$ group. Although **4** has higher reactivity than **3**, its detection limit is bigger than the one of **2**, which prompted us to continue the evaluation at the biological level with probe **2**.

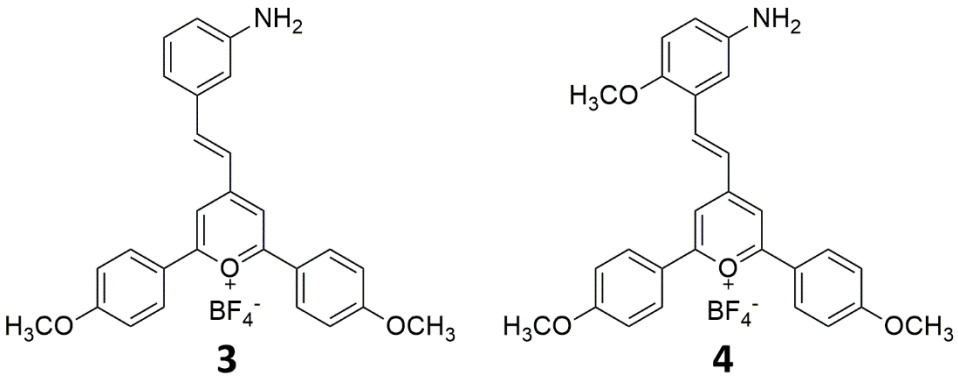

Chart 2. Model compounds **3** and **4** synthesized and studied in the present work.

Once studied the reactivity, sensibility and selectivity of **2** in the *cuvette*, a series of biological assays were conducted. For this, confocal laser scanning microscopy (CLSM) was employed. First, probe **2** was tested for the detection of exogenous NO, using the NO donor S-nitroso-N-acetylpenicillamine (SNAP). Probe **2** was incubated with a culture of human colon carcinoma cells HT-29 and loaded with 100 μM of SNAP. As it can be seen in **Figure 3**, the use of **2** (before addition of the NO donor) affords a negligible background emission, whereas the addition of SNAP lights up the fluorescence at certain areas with a perinuclear location. Flow cytometric analyses confirmed this result (**Figure S7**).

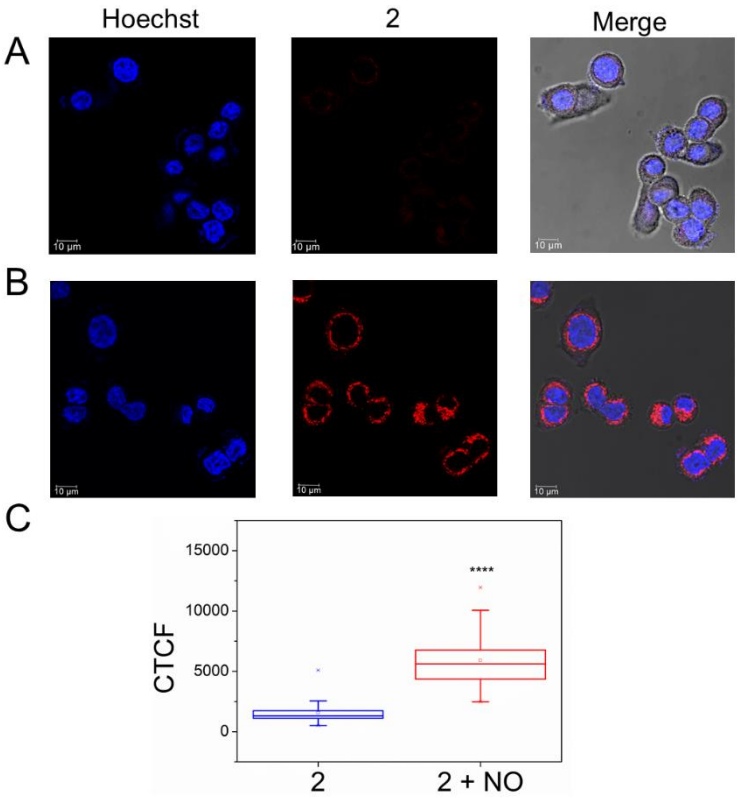

Figure 3. A) HT29 cells stained by **2** (10 µM, 30 min) B) HT29 cells stained by **2** (10 µM, 30 min) and then treated with SNAP (100 µM, 60 min). In all cases, Hoechst (0.1 mg/ml, 5 min) was added to mark nuclei. C) Corrected total cell fluorescence (CFCT) calculated from A and B (red fluorescence). Data are shown as median ± (inter-quartile range) IQR, n=20. Statistical analysis was performed by unpaired t-test (**** indicates a p-value ≤ 0.0001).

According to our previous finding that styrylpyrylium dyes accumulate in the mitochondria efficiently,[19] we hypothesized that the generated signal must arise from such organelle. To confirm the hypothesized mitochondrial nature of the spots, the colocalization with the well-known marker MitoTracker Green FM was assayed. As can be seen in **Figure 4**, the superposition of the emissions is remarkable, with a calculated Pearson's coefficient of 0.94.

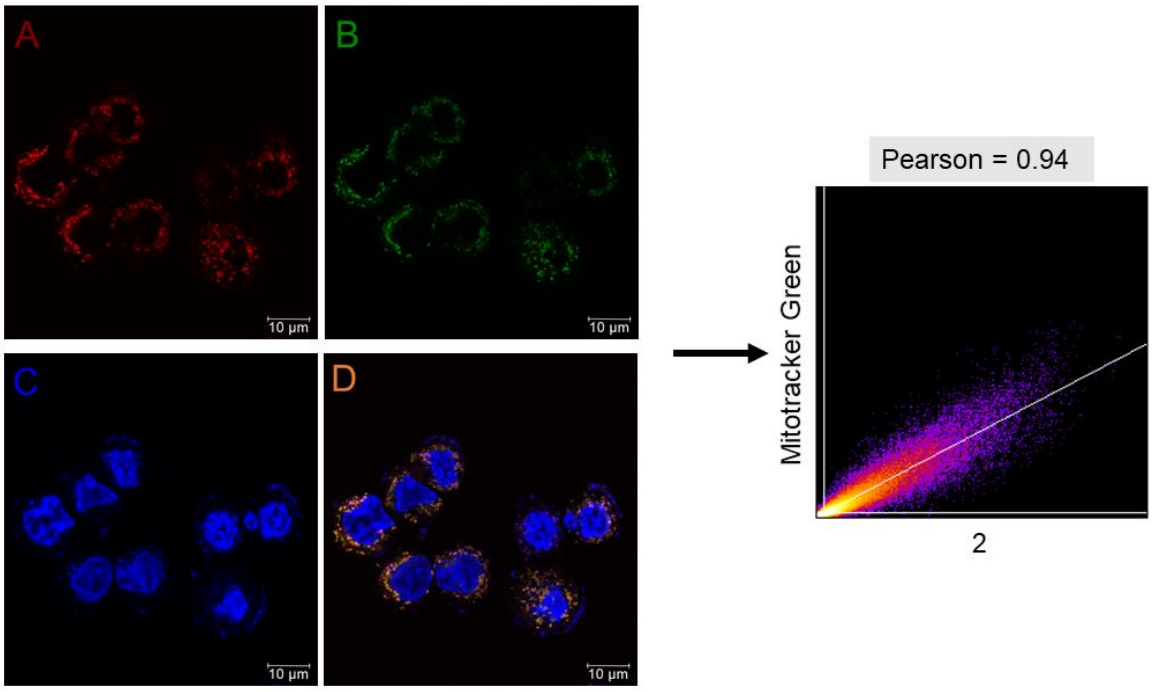

Figure 4. Fluorescence images of HT29 cells coincubated with **2** (10 µM) and Mitotracker Green FM (75 nM) for 30 minutes and then treated with SNAP (100 µM, 60 min). Hoechst (0.1 mg/ml, 5 min) was added to mark nuclei. A) Fluorescent signal of **2**. B) Fluorescent signal of Mitotracker Green FM. C) Fluorescent signal of Hoechst. D) Merged channels.

In the second place, probe **2** was tested for the detection of endogenously generated NO. This assay was carried out using murine RAW 264.7 macrophages, which are very well known for generating NO via the enzyme inducible NO synthase (iNOS) upon stimulation with lipopolysaccharide (LPS).[52] As it can be seen in **Figure 5**, the stimulation with LPS of RAW 264.7 incubated with 10 µM of **2** was followed by an increase of the fluorescence of punctuated areas of the cells imaged by CLSM. Moreover, incubation with the inhibitor of iNOS L-N^G-monomethyl arginine acetate (L-NMMA)[53] resulted in a negligible response to LPS. Analysis by flow cytometry confirmed the CLSM imaging (**Figure S8**). Additionally, toxicity assays were conducted with this cell line, demonstrating that **2** can be used safely at high concentrations (**Figure S9**).

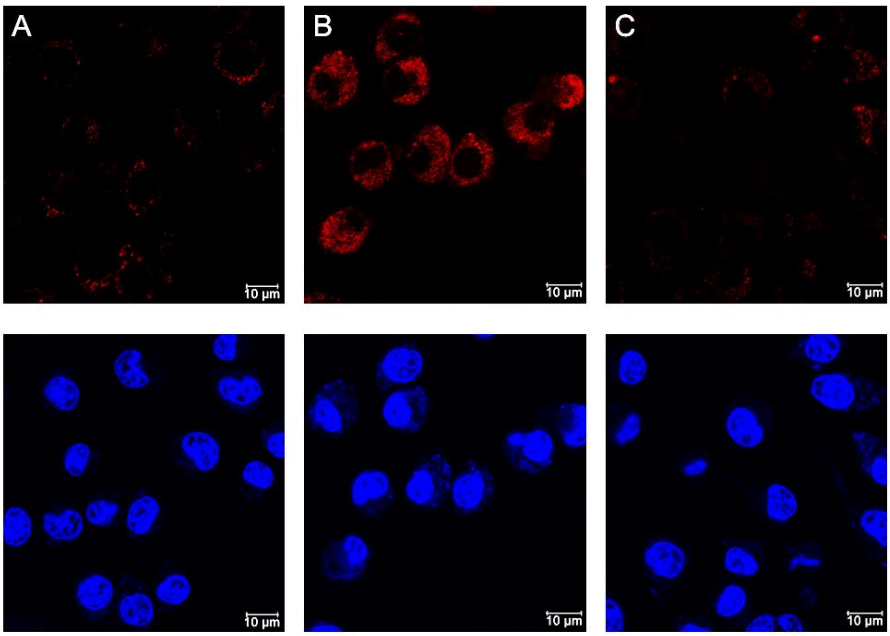

Figure 5. A) RAW 264.7 cells stained by **2** (10 µM, 30 min) B) RAW 264.7 cells stained by **2** (10 µM, 30 min) after the treatment with LPS (20 µg/ml, overnight) C) RAW 264.7 cells stained by **2** (10 µM, 30 min) after the treatment with LPS (20 µg/ml, overnight) and L-NMMA (50 µM, overnight). In all cases, Hoechst (0.1 mg/ml, 5 min) was added to mark nuclei. Top: fluorescent signal of **2**; bottom: fluorescent signal of Hoechst.

Finally, the probe was assayed in a much more complex environment (whole peripheral blood) using flow cytometry as the bioanalytical tool. This type of test is original within the field of NO-probes since biological assays in this area are normally limited to controlled conditions such as cellular cultures. The aim of this new assay was carried out to demonstrate that **2** could extract information from a sample containing leukocytes of different nature (neutrophils, monocytes, NK, B and T cells). Thus, **2** was incubated with human peripheral blood samples extracted from healthy donors. The fluorescence of leukocyte subsets was then analyzed by flow cytometry using two different lasers as excitation sources of **2** (405 nm and 488 nm). The sample was stimulated with LPS to trigger an inflammatory response and monitored over time. As it can be seen in **Figure 6A**, the response of phagocytes (neutrophils and monocytes) is notable, with relative fluorescence signals about one order of magnitude higher than that of lymphocytes (NK, B and T cells). In neutrophils, NO levels were similar ex-vivo

(MFI = 186) and after 24 hours (MFI = 208) of LPS stimulation. However, they were higher after 48 hours of stimulation (MFI = 404). In monocytes, the level of NO progressively increased from ex-vivo (MFI = 113), to 24 (MFI = 344) and 48 (MFI = 719) hours of LPS stimulation. On lymphocytes, only $CD8^+$ T cells showed increasing values of NO levels after 0 (MFI = 10), 24 (MFI = 51) and 48 (MFI = 66) hours of LPS stimulation. Similar results were observed in the PE (586/42 nm) and the V500 (528/45nm) channels.

In the kinetic analysis of the NO levels (**Figure 6B**), compared to cells maintained in RPMI medium, 48 hours of LPS stimulation induced clear increases in the MFI of **2** in neutrophils (maximum reached at 15 minutes), monocytes (maximum reached at 12 minutes) and non-classical $CD16^+$ monocytes (maximum reached at 18 minutes). Very low increases were observed for NK and $CD8^+$ T cells. Overall, the higher response of the neutrophils and monocytes is the expected one since these cells are efficient producers of NO upon stimulation, due to their phagocytic function.[54,55]

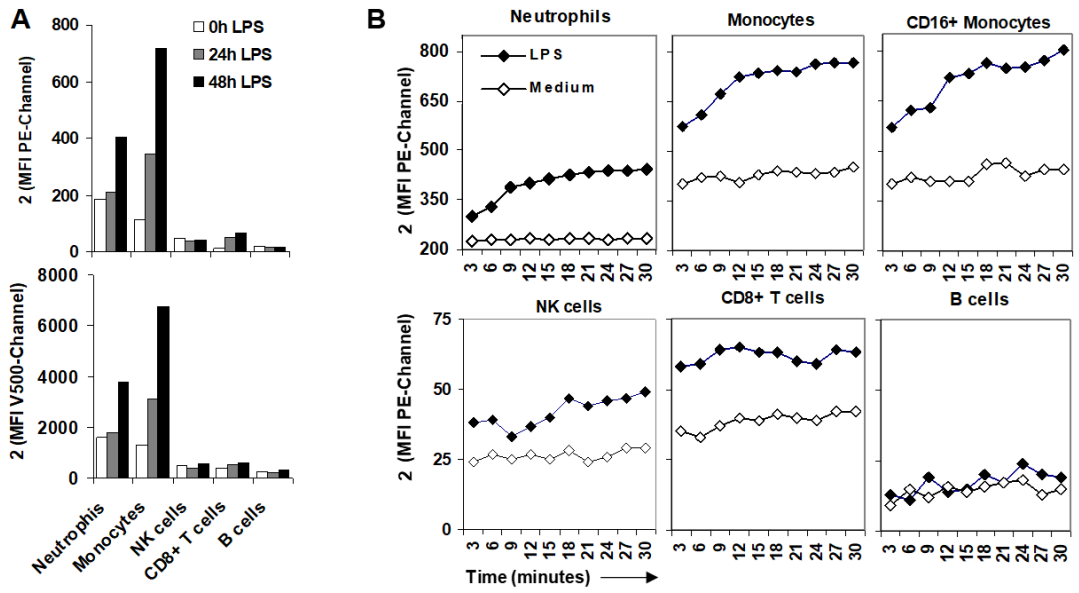

Figure 6. A) Mean fluorescence intensity (MFI) of 10 µM solutions of **2** in leukocyte and lymphocyte subsets assayed by incubating whole peripheral blood diluted 1:1 in RPMI-1640 in a culture incubator for 30 minutes. Blood cells were previously stimulated with 1 µM lipopolysaccharide (LPS) for 30 minutes, 24h or 48h. Fluorescence of **2** was evaluated in the PE-channel (586/42 nm) excited by the blue laser (488nm) and in the V510-channel (528/45) excited by the violet laser (405nm). B) MFI kinetic analysis of **2** in the 30 minutes acquisition time for leukocyte and lymphocyte subsets after 48 h incubation at 37 °C with medium (RPMI) or LPS 1 µg/ml. Results of one representative experiment out of three.

Conclusions

In summary, compound **2** (mtNOpy) has been synthesized and characterized. Its fluorescence has been found to be responsive (turn-on) to nitric oxide (aerated medium) with a detection limit of 88 nM and shows no interference with other RNS, ROS and DHA. The reaction takes place via a deamination process as demonstrated by HRMS. The responsiveness to exogenous (SNAP) and endogenous (LPS induced) NO has been demonstrated in cultured cells (HT-29 and RAW264.7) and mitochondria have been found as the site of the location of this probe (colocalization with Mitotracker Green FM). This is remarkable since most of the reported probes to measure NO at the mitochondria use the TPP cation as a vector. Biological measurements are also carried

out in a real sample of peripheral blood, in which it has been able to discriminate those cells known for producing high levels of NO (neutrophils and monocytes) from those cells with lower activity in this regard (NK, B and T cells). Beyond the specific performance of **2** as a probe for mNO, the relevance of our research lies in the fact that simple modifications of pyrylium dyes could potentially lead to mitochondrial fluorescent sensors for other mitochondrial species (for instance, using boronate groups for hydrogen peroxide or thiol-reactive groups for glutathione), without using TPP as directing group. We hope that the probe here reported, or analogous ones could help to shed some light on the complex biochemistry of NO in mitochondria, especially on currently conflictive aspects regarding this organelle, such as the roles of the controversial mitochondrial NO synthase (mtNOS) or the process of NO-induced mitochondrial biogenesis.[56] Apart from expanding the basic knowledge on mitochondria, styrylpyrylium dyes like the one here reported could be potentially useful for the molecular tracking and imaging of inflammatory cells[57] and hence could orient decision-making processes affecting therapeutic treatments.[58]

Conflicts of interest

There are no conflicts to declare.

Acknowledgements

The authors acknowledge the financial support from Generalitat Valenciana (FG for grant AICO/2020/322 and IMR for Santiago Grisolía fellowship GRISOLIAP/2018/071). SCIC from UJI is acknowledged for technical support.

References

1 S. S. Sabharwal and P. T. Schumacker, Mitochondrial ROS in cancer: initiators, amplifiers or an Achilles' heel?, *Nat. Rev. Cancer*, 2014, **14**, 709–721.

2 M. P. Murphy and R. C. Hartley, Mitochondria as a therapeutic target for common pathologies, *Nat. Rev. Drug Discov.*, 2018, **17**, 865–886.

3 B. Kalyanaraman and J. Zielonka, Small-molecule luminescent probes for the detection of cellular oxidizing and nitrating species, *Free Radic. Biol. Med.*, 2018, **128**, 3–22.

4 E. Ramond, A. Jamet, M. Coureuil and A. Charbit, Pivotal role of mitochondria in macrophage response to bacterial pathogens, *Front. Immunol.*, 2019, **10**, 1–11.

5 E. Shekhova, Mitochondrial reactive oxygen species as major effectors of antimicrobial immunity, *PLoS Pathog.*, 2020, **16**, 1–6.

6 L. D. Lavis, Chemistry Is Dead. Long Live Chemistry!, *Biochemistry*, 2017, **56**, 5165–5170.

7 G. Rong, S. R. Corrie and H. A. Clark, In Vivo Biosensing: Progress and Perspectives, *ACS Sensors*, 2017, **2**, 327–338.

8 W. Xu, Z. Zeng, J. H. Jiang, Y. T. Chang and L. Yuan, Discerning the Chemistry in Individual Organelles with Small-Molecule Fluorescent Probes, *Angew. Chemie - Int. Ed.*, 2016, **55**, 13658–13699.

9 P. Gao, W. Pan, N. Li and B. Tang, Fluorescent probes for organelle-targeted bioactive species imaging, *Chem. Sci.*, 2019, **10**, 6035–6071.

10 J. Li, N. Kwon, Y. Jeong, S. Lee, G. Kim and J. Yoon, Aggregation-Induced Fluorescence Probe for Monitoring Membrane Potential Changes in Mitochondria, *ACS Appl. Mater. Interfaces*, 2018, **10**, 12150–12154.

11 J. Zielonka, J. Joseph, A. Sikora, M. Hardy, O. Ouari, J. Vasquez-Vivar, G. Cheng, M. Lopez and B. Kalyanaraman, Mitochondria-Targeted

Triphenylphosphonium-Based Compounds: Syntheses, Mechanisms of Action, and Therapeutic and Diagnostic Applications, *Chem. Rev.*, 2017, **117**, 10043–10120.

12 C. Ma, F. Xia and S. O. Kelley, Mitochondrial Targeting of Probes and Therapeutics to the Powerhouse of the Cell, *Bioconjug. Chem.*, 2020, **31**, 2650–2667.

13 C. W. T. Leung, Y. Hong, S. Chen, E. Zhao, J. W. Y. Lam and B. Z. Tang, A photostable AIE luminogen for specific mitochondrial imaging and tracking, *J. Am. Chem. Soc.*, 2013, **135**, 62–65.

14 M. H. Lee, N. Park, C. Yi, J. H. Han, J. H. Hong, K. P. Kim, D. H. Kang, J. L. Sessler, C. Kang and J. S. Kim, Mitochondria-Immobilized pH-Sensitive Off − On Fluorescent Probe, *J. Am. Chem. Soc.*, 2014, **136**, 14136–14142.

15 C. J. Zhang, J. Wang, J. Zhang, Y. M. Lee, G. Feng, T. K. Lim, H. M. Shen, Q. Lin and B. Liu, Mechanism-Guided Design and Synthesis of a Mitochondria-Targeting Artemisinin Analogue with Enhanced Anticancer Activity, *Angew. Chemie - Int. Ed.*, 2016, **55**, 13770–13774.

16 H. S. Jung, J. H. Lee, K. Kim, S. Koo, P. Verwilst, J. L. Sessler, C. Kang and J. S. Kim, A Mitochondria-Targeted Cryptocyanine-Based Photothermogenic Photosensitizer, *J. Am. Chem. Soc.*, 2017, **139**, 9972–9978.

17 P. Yuan, X. Mao, X. Wu, S. S. Liew, L. Li and S. Q. Yao, Mitochondria-Targeting, Intracellular Delivery of Native Proteins Using Biodegradable Silica Nanoparticles, *Angew. Chemie*, 2019, **131**, 7739–7743.

18 C. Sun, Z. Wang, L. Yue, Q. Huang, Q. Cheng and R. Wang, Supramolecular induction of mitochondrial aggregation and fusion, *J. Am. Chem. Soc.*, 2020, **142**, 16523–16527.

19 I. Muñoz Resta, F. Lucantoni, N. Apostolova and F. Galindo, Fluorescent styrylpyrylium probes for the imaging of mitochondria in live cells, *Org. Biomol. Chem.*, 2021, DOI: 10.1039/D1OB01543E.

20 F. Galindo, N. Kabir, J. Gavrilovic and D. A. Russell, Spectroscopic studies of 1,2-diaminoanthraquinone (DAQ) as a fluorescent probe for the imaging of nitric oxide in living cells, *Photochem. Photobiol. Sci.*, 2007, **7**, 126–130.

21 M. J. Marín, P. Thomas, V. Fabregat, S. V. Luis, D. A. Russell and F. Galindo, Fluorescence of 1,2-diaminoanthraquinone and its nitric oxide reaction product within macrophage cells, *ChemBioChem*, 2011, **12**, 2471–2477.

22 A. Beltrán, M. Isabel Burguete, D. R. Abánades, D. Pérez-Sala, S. V. Luis and F. Galindo, Turn-on fluorescent probes for nitric oxide sensing based on the ortho-hydroxyamino structure showing no interference with dehydroascorbic acid, *Chem. Commun.*, 2014, **50**, 3579–3581.

23 R. Radi, Oxygen radicals, nitric oxide, and peroxynitrite: Redox pathways in molecular medicine, *Proc. Natl. Acad. Sci. U. S. A.*, 2018, **115**, 5839–5848.

24 H. Kojima, N. Nakatsubo, K. Kikuchi, S. Kawahara, Y. Kirino, H. Nagoshi, Y. Hirata and T. Nagano, Detection and Imaging of Nitric Oxide with Novel Fluorescent Indicators: Diaminofluoresceins, *Anal. Chem.*, 1998, **70**, 2446–2453.

25 H. Kojima and T. Nagano, Fluorescent indicators for nitric oxide, *Angew. Chemie - Int. Ed.*, 1999, **38**, 3209–3212.

26 P. R. Escamilla, Y. Shen, Q. Zhang, D. S. Hernandez, C. J. Howard, X. Qian, D. Y. Filonov, A. V. Kinev, J. B. Shear, E. V. Anslyn and Y. Yang, 2-Amino-3′-dialkylaminobiphenyl-based fluorescent intracellular probes for nitric oxide surrogate N_2O_3, *Chem. Sci.*, 2020, **11**, 1394–1403.

27 X. Chen, F. Wang, J. Y. Hyun, T. Wei, J. Qiang, X. Ren, I. Shin and J. Yoon,

Recent progress in the development of fluorescent, luminescent and colorimetric probes for detection of reactive oxygen and nitrogen species, *Chem. Soc. Rev.*, 2016, **45**, 2976–3016.

28 L. Wang, J. Zhang, X. An and H. Duan, Recent progress on the organic and metal complex-based fluorescent probes for monitoring nitric oxide in living biological systems, *Org. Biomol. Chem.*, 2020, **18**, 1522–1549.

29 X. Ye, S. S. Rubakhin and J. V. Sweedler, Detection of nitric oxide in single cells, *Analyst*, 2008, **133**, 423–433.

30 T. Nagano and T. Yoshimura, Bioimaging of nitric oxide, *Chem. Rev.*, 2002, **102**, 1235–1269.

31 M. H. Lim, D. Xu and S. J. Lippard, Visualization of nitric oxide in living cells by a copper-based fluorescent probe, *Nat. Chem. Biol.*, 2006, **2**, 375–380.

32 Y. Gabe, Y. Urano, K. Kikuchi, H. Kojima and T. Nagano, Highly Sensitive Fluorescence Probes for Nitric Oxide Based on Boron Dipyrromethene Chromophore - Rational Design of Potentially Useful Bioimaging Fluorescence Probe, *J. Am. Chem. Soc.*, 2004, **126**, 3357–3367.

33 Y. Yang, S. K. Seidlits, M. M. Adams, V. M. Lynch, C. E. Schmidt, E. V. Anslyn and J. B. Shear, A highly selective low-background fluorescent imaging agent for nitric oxide, *J. Am. Chem. Soc.*, 2010, **132**, 13114–13116.

34 L. Yuan, W. Lin, Y. Xie, B. Chen and S. Zhu, Single fluorescent probe responds to H_2O_2, NO, and H_2O_2/NO with three different sets of fluorescence signals, *J. Am. Chem. Soc.*, 2012, **134**, 1305–1315.

35 R. Leggett, P. Thomas, M. J. Marín, J. Gavrilovic and D. A. Russell, Imaging of compartmentalised intracellular nitric oxide, induced during bacterial phagocytosis, using a metalloprotein-gold nanoparticle conjugate, *Analyst*, 2017,

142, 4099–4105.

36 C. J. Reinhardt, E. Y. Zhou, M. D. Jorgensen, G. Partipilo and J. Chan, A Ratiometric Acoustogenic Probe for in Vivo Imaging of Endogenous Nitric Oxide, *J. Am. Chem. Soc.*, 2018, **140**, 1011–1018.

37 Q. Han, J. Liu, Q. Meng, Y. L. Wang, H. Feng, Z. Zhang, Z. P. Xu and R. Zhang, Turn-on fluorescence probe for nitric oxide detection and bioimaging in live cells and zebrafish, *ACS Sensors*, 2019, **4**, 309–316.

38 T. Zhou, J. Wang, J. Xu, C. Zheng, Y. Niu, C. Wang, F. Xu, L. Yuan, X. Zhao, L. Liang and P. Xu, A Smart Fluorescent Probe for NO Detection and Application in Myocardial Fibrosis Imaging, *Anal. Chem.*, 2020, **92**, 5064–5072.

39 T. W. Shiue, Y. H. Chen, C. M. Wu, G. Singh, H. Y. Chen, C. H. Hung, W. F. Liaw and Y. M. Wang, Nitric oxide turn-on fluorescent probe based on deamination of aromatic primary monoamines, *Inorg. Chem.*, 2012, **51**, 5400–5408.

40 Y. Huo, J. Miao, Y. Li, Y. Shi, H. Shi and W. Guo, Aromatic primary monoamine-based fast-response and highly specific fluorescent probes for imaging the biological signaling molecule nitric oxide in living cells and organisms, *J. Mater. Chem. B*, 2017, **5**, 2483–2490.

41 H. Yu, X. Zhang, Y. Xiao, W. Zou, L. Wang and L. Jin, Targetable fluorescent probe for monitoring exogenous and endogenous NO in mitochondria of living cells, *Anal. Chem.*, 2013, **85**, 7076–7084.

42 X. Zhu, J. Q. Chen, C. Ma, X. Liu, X. P. Cao and H. Zhang, A ratiometric mitochondria-Targeting two-photon fluorescent probe for imaging of nitric oxide in vivo, *Analyst*, 2017, **142**, 4623–4628.

43 C. Gao, L. Lin, W. Sun, Z. L. Tan, J. R. Huang, L. He and Z. L. Lu,

Dihydropyridine-derived BODIPY probe for detecting exogenous and endogenous nitric oxide in mitochondria, *Talanta*, 2018, **176**, 382–388.

44 Y. Huo, J. Miao, J. Fang, H. Shi, J. Wang and W. Guo, Aromatic secondary amine-functionalized fluorescent NO probes: improved detection sensitivity for NO and potential applications in cancer immunotherapy studies, *Chem. Sci.*, 2019, **10**, 145–152.

45 Z. Yu, J. Zhou, X. Dong, W. Zhao and Z. Chen, Visualizing Nitric oxide in mitochondria and lysosomes of living cells with N-Nitrosation of BODIPY-based fluorescent probes, *Anal. Chim. Acta*, 2019, **1067**, 88–97.

46 Y. Q. Sun, J. Liu, H. Zhang, Y. Huo, X. Lv, Y. Shi and W. Guo, A mitochondria-targetable fluorescent probe for dual-channel no imaging assisted by intracellular cysteine and glutathione, *J. Am. Chem. Soc.*, 2014, **136**, 12520–12523.

47 C. Wang, X. Song, Z. Han, X. Li, Y. Xu and Y. Xiao, Monitoring Nitric Oxide in Subcellular Compartments by Hybrid Probe Based on Rhodamine Spirolactam and SNAP-tag, *ACS Chem. Biol.*, 2016, **11**, 2033–2040.

48 J. Tang, Z. Guo, Y. Zhang, B. Bai and W. H. Zhu, Rational design of a fast and selective near-infrared fluorescent probe for targeted monitoring of endogenous nitric oxide, *Chem. Commun.*, 2017, **53**, 10520–10523.

49 C. Li, W. J. Tang, W. Feng, C. Liu and Q. H. Song, A rapid-response and ratiometric fluorescent probe for nitric oxide: From the mitochondria to the nucleus in live cells, *Anal. Chim. Acta*, 2020, **1096**, 148–158.

50 X. Zhang, W. S. Kim, N. Hatcher, K. Potgieter, L. L. Moroz, R. Gillette and J. V. Sweedler, Interfering with nitric oxide measurements. 4,5-Diaminofluorescein reacts with dehydroascorbic acid and ascorbic acid, *J. Biol. Chem.*, 2002, **277**, 48472–48478.

51 C. Felip-León, C. A. Angulo-Pachón, J. F. Miravet and F. Galindo, Self-Assembly Controls Reactivity with Nitric Oxide: Implications for Fluorescence Sensing, *ACS Omega*, 2018, **3**, 15538–15545.

52 V. Vijayan, P. Pradhan, L. Braud, H. R. Fuchs, F. Gueler, R. Motterlini, R. Foresti and S. Immenschuh, Human and murine macrophages exhibit differential metabolic responses to lipopolysaccharide - A divergent role for glycolysis, *Redox Biol.*, 2019, **22**, 101147.

53 D. D. Rees, R. M. J. Palmer, R. Schulz, H. F. Hodson and S. Moncada, Characterization of three inhibitors of endothelial nitric oxide synthase in vitro and in vivo, *Br. J. Pharmacol.*, 1990, **101**, 746–752.

54 G. Laffi, M. Foschi, E. Masini, A. Simoni, L. Mugnai, G. La Villa, G. Barletta, P. F. Mannaioni and P. Gentilini, Increased production of nitric oxide by neutrophils and monocytes from cirrhotic patients with ascites and hyperdynamic circulation, *Hepatology*, 1995, **22**, 1666–1673.

55 N. C. C. Schachnik, V. Peruhype-Magalhães, G. M. M. Paula, F. Lucas, V. M. Freitas, O. A. Martins-Filho and L. M. S. Dusse, Intracellular nitric oxide assessment in whole blood leukocytes by flow cytometry: Optimization and applicability to monitor patients with chronic graft nephropathy, *J. Immunol. Methods*, 2009, **343**, 103–111.

56 C. H. Tengan and C. T. Moraes, NO control of mitochondrial function in normal and transformed cells, *Biochim. Biophys. Acta - Bioenerg.*, 2017, **1858**, 573–581.

57 A. Fernández and M. Vendrell, Smart fluorescent probes for imaging macrophage activity, *Chem. Soc. Rev.*, 2016, **45**, 1182–1196.

58 G. P. Birch, T. Campbell, M. Bradley and K. Dhaliwal, Optical Molecular Imaging of Inflammatory Cells in Interventional Medicine–An Emerging

Strategy, *Front. Oncol.*, 2019, **9**, 882.